

Article

Utility Paths Combination in HEN for Energy Saving and CO₂ Emission Reduction

Abdelbagi Osman ^{1,2,*}, Mohanad Eltayeb ² and Fahd Rajab ¹

¹ Department of Chemical Engineering, College of Engineering, Najran University, P.O. Box 1988 Najran, Saudi Arabia

² Department of Chemical Engineering and Chemical Technology, Faculty of Engineering and Technology, University of Gezira, P.O. Box 20 Wad Medani, Sudan

* Correspondence: aomustafa@nu.edu.sa

Received: 15 April 2019; Accepted: 1 July 2019; Published: 4 July 2019



Abstract: Energy demand and flue gas emissions, namely carbon dioxide (CO₂) associated with the industrial revolution have exhibited a continuous rise. Several approaches were introduced recently to mitigate energy consumption and CO₂ emissions by either grass root design or retrofit of existing heat exchanger networks (HEN) in chemical process plants. In this work, a combinatorial approach of path combination is used to generate several options for heat recovery enhancement in HEN. The options are applied to successively shift heat load from HEN utilities using combined utility paths at different heat recovery approach temperature (HRAT) considering exchangers pressure drop. Industrial case study for HEN of the preheat train in crude oil distillation unit from the literature is used to demonstrate the approach. The obtained results have been studied economically using the cost targeting of Pinch Technology. As a result, both external energy usage and CO₂ emissions have been reduced from a heater device in HEN by 20% and 17%, respectively, with a payback of less than one year.

Keywords: HEN retrofit; path analysis; paths combination; energy saving; CO₂ emission

1. Introduction

Energy demand has prompted different approaches recently due to limited energy resources as well as technical and environmental constraints. As fossil fuel sources are depleting, energy optimization and upgrades of plants have become crucial to narrow the gap between energy supply and demand. In the literature, there are various strategies to achieve energy optimization in industrial processes. Research and development units in the industry are focusing on maximizing individual units' throughputs following local and global economics. However, due to operational and forecasting constraints, they are faced with challenging trade-offs. As a result, retrofit of existing plants offers a viable alternative to overcome operational requirements.

Retrofit plans in heat exchanger networks (HEN) include reducing the use of utilities, upgrading heat transfer units, installing additional heat transfer area, re-piping streams and re-assigning new heat recovery matches. HEN is a heat recovery system that enables heat exchange between hot and cold streams in chemical process plants, which is essential for energy conservation within a plant. The grass-roots design of HEN as studied by Linnhoff et al. has been significantly improved through the use of Pinch Technology [1–3]. Tjoe and Linnhoff were the first to propose a systematic methodology for heat exchanger network retrofit using pinch analysis [4], based on the elimination of any cross-pinch match by disconnecting units that transfer heat across the pinch. Gadalla et al. have presented a methodology to maximize the use of existing equipment in HEN and distillation column based on rigorous simulation and optimization framework using pinch analysis [5]. Biyanto et al.

have recently conducted a HEN retrofit for maximum energy recovery without topological changes using a genetic algorithm (GA) to screen different optimization scenarios for selecting optimum heat transfer coefficient [6]. A step-wise approach for optimal HEN retrofit to reduce calculation times and annualized cost associated with HEN complexity has recently introduced by Ayotti-Sauve et al. [7]. Kang and Liu have conducted a comprehensive review and analysis for the synthesis of flexible HEN, including both grass-roots and retrofit design [8].

Different methodologies have been developed based on the concept of utility path analysis in HEN such as those developed by Varbanov and Makwana [9], where they first presented the rule of path construction for HEN retrofit. Van Reisen et al. have proposed a method of path analysis for decomposition and prescreening of HEN [10]. Their technique selects and evaluates only potential subnetwork parts of the existing HEN. In subsequent work, Van Reisen et al. have presented an extension to the path analysis procedure, by considering structural interconnections while solving the retrofit problem [11]. They divided the network into many sub-networks by a combination of structural units using path analysis. These units, called zones, must be as self-contained as possible, similar to the approach used in grass-root problems. Paths help to classify the zones that are better suitable to include structural modifications. The refined path zones are based on functions of plant sections as well as operational constraints such as temperature range of process streams. For enhancing the process-to-process heat recovery in HEN, Osman et al. have introduced a combinatorial approach of paths combination [12]. Their strategy depends on shifting heat loads through utility paths at the constraint of heat recovery approach temperature (HRAT) and exchanger pressure drop. In subsequent work, Osman et al. applied the same methodology to screen more extensive options of heat recovery enhancement in HEN with an option of varying HEN streams temperature [13].

Awad and Abdelgadir have conducted two different studies for energy saving in HEN of crude oil pre-heat train unit using the paths combination approach. However, they did not consider the effect of pressure drop while estimating the heat transfer coefficient in HEN devices [14,15]. They also ignored the emission of CO₂, although the main heater of the network is using heavy fuel.

HEN Retrofit study considering the constraints of the pressure drop in HEN was first recognized by Polley et al. [16]. Comprehensive research considering the pressure drop in HEN retrofit was conducted by Panjehshahi [17], Marcone et al. [18] and Gadalla [19].

Regarding HEN area distribution, along with economic assessment, Lai et al. have introduced a recent study where they presented a new customized approach for HEN retrofit [20]. They used a combination of individual stream temperature versus enthalpy to map hot and cold streams to minimize the overall heat exchanger area. They also used graphical cost screening tool and strategies to steer and customize HEN retrofit design toward a desired investment payback period.

Regarding environmental pollution outstretched from process plants, significant efforts and strategies have been made by Steyn [21] and John [22] to provide CO₂ emissions reduction solutions. These strategies include improving the energy efficiency in process plants and fuel switching as well as renewable energy technologies such as carbon capture and storage (CCS). Gadalla et al. have developed a simple approach for optimizing the process conditions of industrial units to reduce its CO₂ emissions and energy demands [5].

Kang and Liu have conducted a recent work by developing a systematic strategy for HEN retrofit to minimize total annual cost and CO₂ emission. Based on a multi-objective optimization model [23].

Most of the previous work conducted for energy saving in process plants were associated with costly topological changes in HEN. Such changes were either addition of new heat exchangers, re-piping or resequencing the existing devices. However, topological changes always require additional space (platform) in the plant, which might be unavailable or/and restricted for safety consideration. Topological changes also associated with civil work and have not been considered in previous studies.

Accordingly, in this work, the authors carried out energy optimization for an existing HEN (crude oil preheat train unit) using the combinatorial approach of path combination. Apart from the previous works of the authors that based on a fixed value of HRAT while ignoring the effect on CO₂ emission,

the current work is conducted at different HRAT values considering the cost targeting approach, exchangers' pressure drop, and the impact of energy saving in HEN on CO₂ emissions.

2. Methods

The method applied for energy saving in HEN in the current study is a combinatorial approach of utility paths combination and cost targeting of pinch technology.

Utility path is an imaginary connection between a heater and a cooler through a definite match(es) in HEN [12]. A certain amount of heat duty can be shifted using the plus-minus principle along the utility path. For instance, if a certain amount of heat duty is to be subtracted from hot and cold utilities using the utility path, it must be added and deducted alternatively to and from the matches on that path.

The approach allows for successive heat load shifting from HEN utilities at the minimum HRAT values to ensure maximum possible heat recovery. Furthermore, the impact of reducing energy consumption on the reduction of flue gas emissions is calculated as a CO₂, emitted from the furnace heater in HEN.

2.1. Path Combination Approach

The approach is typically a combinatorial procedure for screening broader alternatives by combining the available utility paths in HEN systematically to enhance the process-to-process heat recovery with the addition of new heat transfer area [24]. The available utility paths in HEN are combined according to the combination law by Equation (1) [25].

$$C(n, r) = \frac{n!}{(n-r)! \cdot r!} \quad (1)$$

where, C , n , and r : combination, number of paths in the HEN and size of combination, respectively; ($r \leq n$).

For n number of paths in HEN, different sets of combined paths can be generated including available single paths. For example, if 3 paths (A, B, and C) are available in an existing HEN, the possible combinations are a set of unilateral paths (A, B and C) each alone, sets of bilateral combined paths (AB, AC, and BC) and a set of trilateral combined paths (ABC). More detail of path combinations is available in a study introduced by Osman [24].

2.1.1. Heat-Shifting Process

Heat load shifting through utility paths in HEN is constrained by the minimum heat transfer driving force between hot and cold streams of HEN, which is called heat recovery approach temperature (HRAT). To select the most optimum HRAT, a range of several values between 2 °C to 24 °C is considered for this study.

A computer software called Hint, which was presented by Martin and Mato [26], has been used to run the heat-shifting process based on a simple energy balance concept. The Hint software package cannot shift the heat load for combined paths in a simultaneous way. However, it allows selection of each utility path and runs the heat load shifting until temperature driving force reaches the set HRAT value. Heat duties for exchangers, hot and cold utilities for HEN under study, are tabulated in Appendix tables for all the three heat-shifting options at different HRAT values.

2.1.2. Cost Targeting

For the selection of optimum HRAT, the range of HRAT values stated above is analyzed economically based on the cost targeting method of Pinch Technology [2,3].

The cost targeting depends on operating, annualized capital, and total costs. The operating cost for a new situation after heat-shifting is estimated by Equations (2)–(4).

$$\text{Operating}_{\text{cost}} = \sum HU_{\text{new.cost}} + \sum CU_{\text{new.cost}} \quad (2)$$

$$HU_{\text{new.cost}} = Q_{\text{new.H}} \cdot HU_{\text{price}} \quad (3)$$

$$CU_{\text{new.cost}} = Q_{\text{new.C}} \cdot CU_{\text{price}} \quad (4)$$

where $HU_{\text{new.cost}}$ and $CU_{\text{new.cost}}$ represent the costs for hot and cold utilities after heat-shifting (\$/yr). HU_{price} and CU_{price} are hot and cold utility prices, respectively (\$/kW.yr). $Q_{\text{new.H}}$ and $Q_{\text{new.C}}$ are the new (after heat-shifting) hot and cold utility heat duty (kW), respectively.

For the annualized capital cost, the required additional heat transfer area due to heat-shifting process needs to be determined. Therefore, a new heat transfer area for each affected exchanger in HEN can be first predicted according to the following Equation (5)

$$\frac{A_{\text{before}}}{A_{\text{after}}} = \frac{Q_{\text{before}}}{Q_{\text{after}}} \quad (5)$$

where A_{before} , Q_{before} , A_{after} , Q_{after} are exchanger heat transfer area (m^2) and heat load (kW) before and after heat-shifting process, respectively.

The initial result from heat transfer area is used in the pressure drop correlations for shell and tube heat exchanger developed by Nie and Zhu [27]. Existing pressure drop for each exchanger is maintained to avoid extra pumping cost for HEN streams. Pressure drop is used to obtain the heat transfer coefficients h_T and h_S for tube and shell side, respectively, using Equations (6) and (7).

$$\Delta P_T = K_{PT1} \cdot A \cdot h_T^{3.5} + K_{PT2} \cdot h_T^{2.5} \quad (6)$$

$$\Delta P_S = K_{S1} \cdot h_S^{2.86} + K_{S2} \cdot A \cdot h_S^{4.42} + K_{S3} \cdot A \cdot h_S^{4.69} \quad (7)$$

where A is the predicted heat transfer area of the exchanger (m^2). ΔP_T and ΔP_S are pressure drop for tube and shell sides of the exchangers (kPa), respectively. K_{PT1} and K_S are dimensional constants for tube and shell sides of the exchanger, respectively. These constants are functions of fluids' physical properties and exchanger's geometrical configuration. More details about these constants are available in the Appendix A.

Due to the complexity of the above two correlations where both h_T and h_S are raised to a fractional power, they are solved using Mathcad software. The values of h_T and h_S for the affected exchangers in HEN are tabulated in Appendix A, Table A10 for all the heat-shifting options.

Based on the obtained heat transfer coefficient, the actual heat transfer area for each exchanger is calculated by the area targeting Equation (8).

$$A = \left(\frac{1}{h_T} + \frac{1}{h_S} \right) \times \frac{Q}{LMTD \times F_T} \quad (8)$$

where Q is the heat duty (kW) for each exchanger, and it is found from the energy balance Equation (9).

$$Q = \dot{m} C_p \Delta T \quad (9)$$

where \dot{m} is the stream mass flow rate (kg/s), C_p is the stream heat capacity (kW/kg.°C), and ΔT is the inlet and outlet temperature difference (°C). The correction factor (F_T) is usually ranged between (0.0

and 1.0). However, in the present case, it is assumed to be 1.0. The logarithmic mean temperature difference *LMTD* is calculated as follows:

$$LMTD = \left(\frac{\Delta T1 - \Delta T2}{\ln\left(\frac{\Delta T1}{\Delta T2}\right)} \right) \quad (10)$$

$$\Delta T1 = T_{H,in} - T_{C,out} \quad (11)$$

$$\Delta T2 = T_{H,out} - T_{C,in} \quad (12)$$

where $\Delta T1$, $\Delta T2$ are exchanger hot side and cold side temperature difference, respectively. $T_{H,in}$, $T_{H,out}$, $T_{C,in}$, $T_{C,out}$ are exchanger's hot inlet, hot outlet, cold inlet and cold outlet temperature ($^{\circ}\text{C}$), respectively.

For estimating the annualized capital cost, capital investment should be calculated first using Equations (13)–(16):

$$\text{Capital Investment} = \Delta N \left(a + b \left(\frac{\Delta A}{\Delta N} \right)^c \right) \quad (13)$$

$$\Delta N = \frac{\Delta A}{av_{shell}} \quad (14)$$

$$av_{shell} = \frac{A_{ex.HEN}}{N_{shell}} \quad (15)$$

$$\Delta A = A_{new.HEN} - A_{ex.HEN} \quad (16)$$

where $A_{ex.HEN}$, $A_{new.HEN}$ and ΔA denote existing, new and additional exchanger heat transfer area (m^2), respectively, whereas ΔN , av_{shell} , and N_{shell} indicate the number of required extra shells, the average size of exchangers shell and number of exchanger shells, respectively. The values of cost coefficients a , b , and c are 33422, 814, and 0.81, respectively, for carbon steel exchanger. The data for heat duties and exchangers' heat transfer area are tabulated in the Appendix tables for all heat-shifting options.

Annualized capital and total annual costs are calculated using Equations (17) and (18), respectively. It is assumed that the capital has been borrowed over a fixed period at a fixed interest rate.

$$\text{Annual capital cost} = \text{capital investment} \times \frac{i(1+i)^n}{(1+i)^n - 1} \quad (17)$$

$$\text{Total annual cost} = \text{annual capital cost} + \text{operating cost} \quad (18)$$

where i and n represent the fractional interest rate per year, and several years and are assumed to be 0.15/year and 2 years, respectively. The total annual cost changes according to the values of HRAT. The optimum HRAT is obtained at the point of the minimum total annual cost.

2.1.3. Economic Assessment

Economic analysis is conducted based on the amount of savings (\$/yr), capital investment (\$), and payback period (yr). As per Al-Riyami et al. [28], saving, investment, and payback period are calculated based on the following assumptions:

- Investment is considered only for the required additional area.
- No piping or other costs are considered.
- The cost of hot and cold utility is fixed.

Saving can be calculated from the Equations (19)–(21) below:

$$\text{Saving}_{cost} = \sum HU_{ex.cost} - \sum HU_{new.cost} + \sum CU_{ex.cost} - \sum CU_{new.cost} \quad (19)$$

$$HU_{ex.cost} = Q_{ex.H} \cdot HU_{price} \quad (20)$$

$$CU_{ex.cost} = Q_{ex.C} \cdot CU_{price} \quad (21)$$

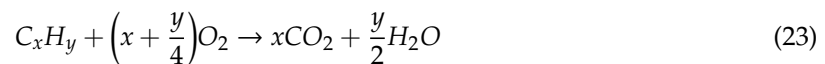
where, $HU_{ex.cost}$ and $CU_{ex.cost}$, are existing (before heat-shifting) hot and cold utility cost (\$/yr), respectively. $Q_{ex.H}$ and $Q_{ex.C}$ are existing (before heat-shifting) hot and cold utility heat duty (kW), respectively. $HU_{new.cost}$ and $CU_{new.cost}$ are presented in Equations (3) and (4) above.

The capital investment cost (\$) for HEN, where an additional area is required, are calculated in Equations (13)–(16) above. The payback period is calculated using Equation (24) below:

$$Payback = \frac{Investment}{Saving} \quad (22)$$

2.1.4. Energy Saving in HEN and CO₂ Emission

CO₂ emissions can be regarded as an additional parameter in search of optimum solution(s). Burning fuel in the presence of excess air results in combustion that produces carbon dioxide and water vapor according to the stoichiometric Equation (23):



where x and y denote the number of carbon C and hydrogen H atoms present in fuel compositions, respectively. To estimate the mass flow rate (M) of emissions ($Mass\ of\ CO_2$) in kg/hr, Equation (24) is adopted from Gadalla et al. [5].

$$M_{CO_2} = \left(\frac{Q_{Fuel}}{NHV}\right) \cdot C\% \cdot \alpha \quad (24)$$

where Q_{Fuel} is fuel heat quantity, calculated by Equation (25), Q_{proc} is the process heat duty of heater in HEN, (η_{Furn} is furnace efficiency, NHV is fuel net heat value, and $C\%$ is the percentage of carbon content in fuel; case study values), and α is the molar mass ratio for CO₂ to C which is 3.67.

$$Q_{Fuel} = \frac{Q_{proc}}{\eta_{Furn}} \quad (25)$$

The overall methodology can be summarized in the flow diagram shown in Figure 1.

3. HEN Case Study

The case study adopted in this work is a HEN for a pre-heat train of a crude oil distillation unit taken from Panjishahi and Tahouni [29], Awad [14] and Abdelgadir [15]. The schematic representation of HEN with stream data (temperature, exchanger heat load, the duty of hot and cold utility, and specific heat mass flow) is shown in Figure 2. The available utility paths in such HEN are identified separately as in Figure 3.

The paths combination approach has been used by Abdelgadir [15] to generate several options of heat-shifting in HEN of a pre-heat train unit while ignoring the exchangers' pressure drop. However, only three options were found feasible in terms of optimum HRAT value. These best options are adopted in this study for further analysis considering exchangers' pressure drop and the effect of energy saving on CO₂ emission. The selected options are listed in Table 1.

Table 1. Paths combination options.

Option No.	Combined Paths
1	A and B
2	B and D
3	A, B, C, D and E

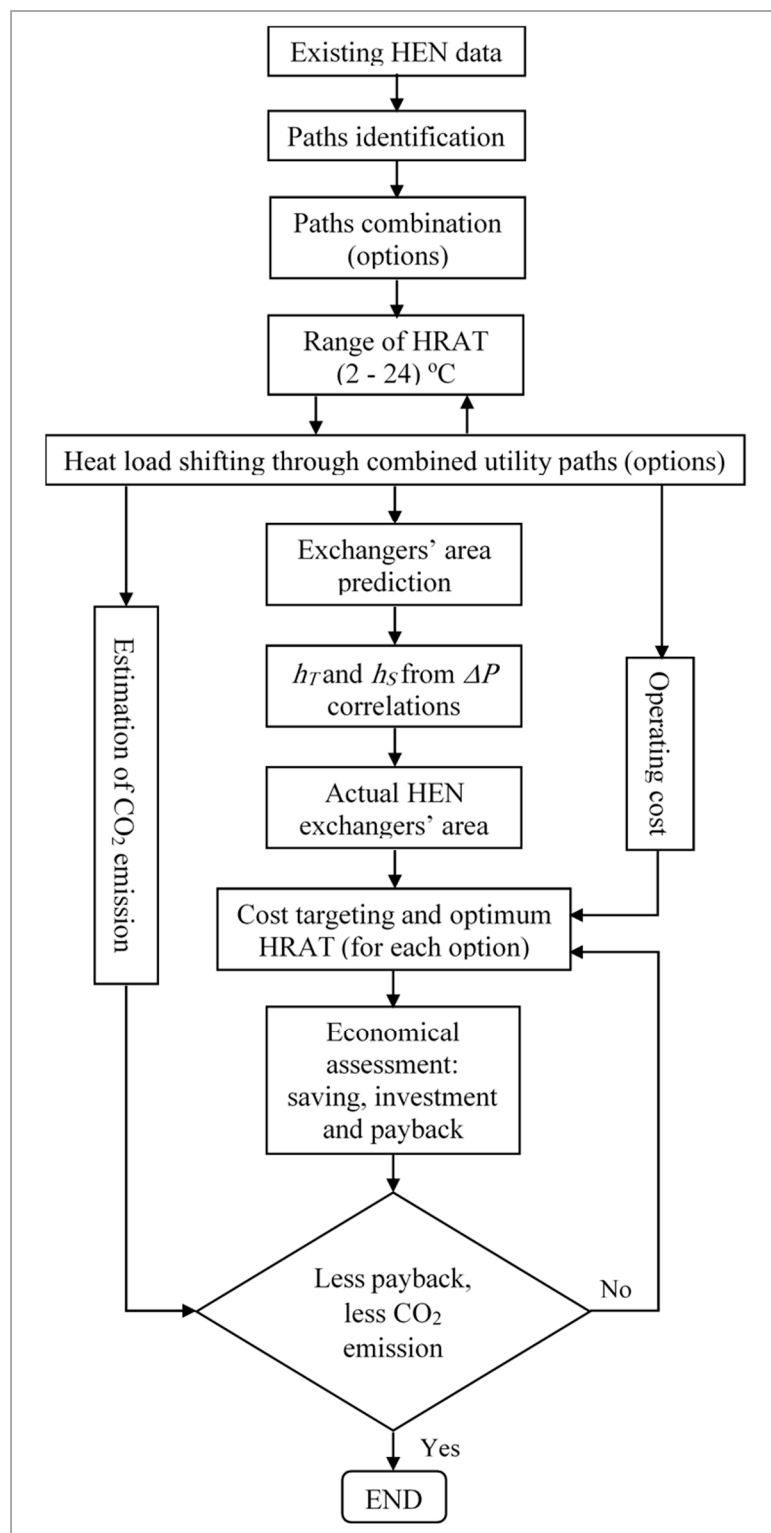


Figure 1. Overall methodology flow diagram.

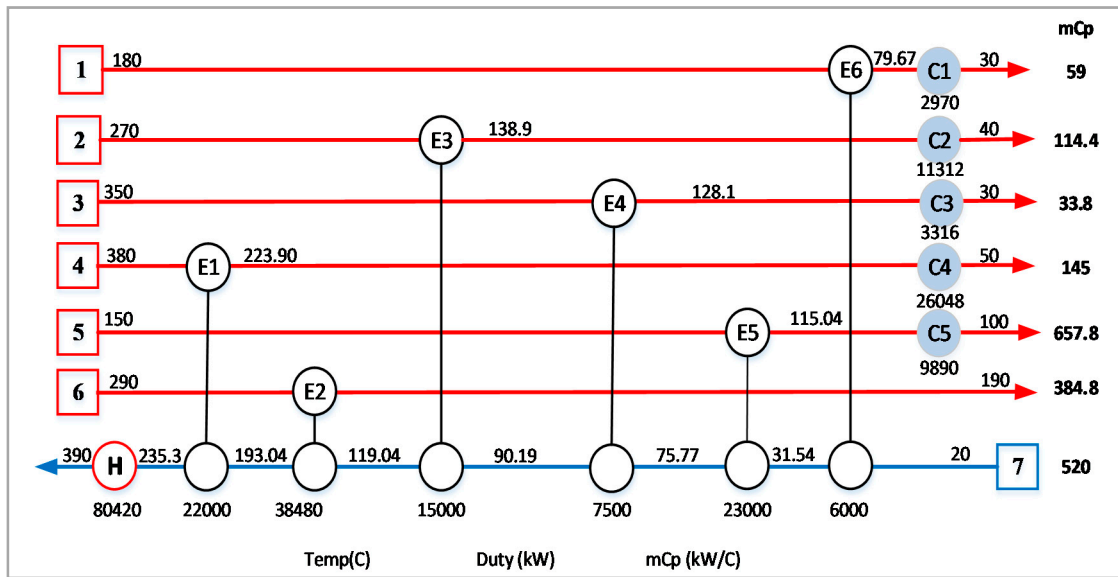


Figure 2. Grid diagram of existing heat exchanger networks (HEN) of crude oil pre-heat train with stream data.

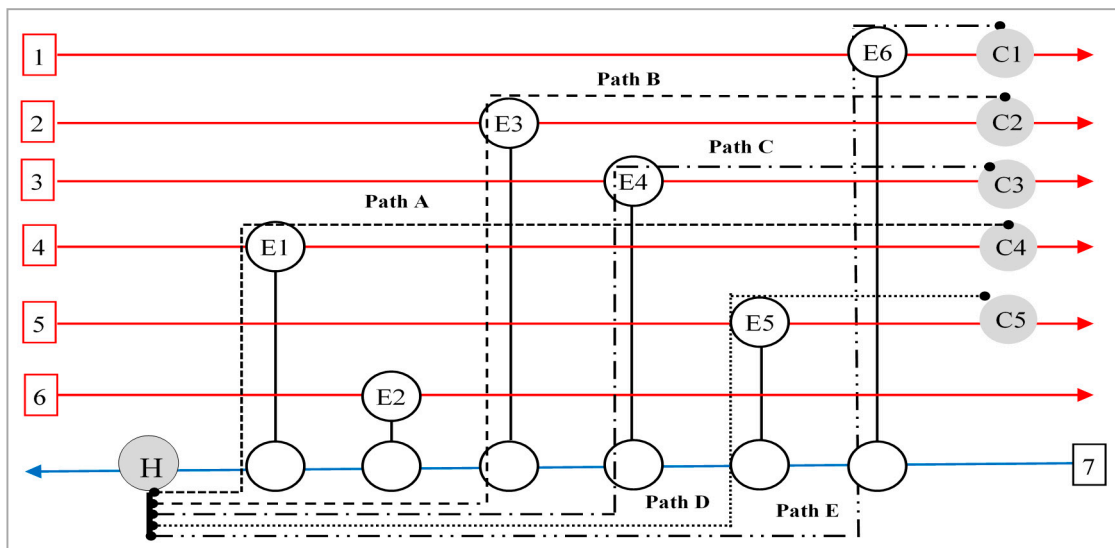


Figure 3. Available individual utility paths in HEN.

According to a previous study by Panjeshahi and Tahouni [29], hot and cold utility prices for the preheat train are tabulated in Table 2:

Table 2. Cost data for crude oil preheat train.

Hot Utility (Furnace)	107 (\$/kW.yr)
Cold Utility	10.7 (\$/kW.yr)

All the data (including equations) required to estimate the heat transfer coefficients for shell and tube sides of the exchangers are available in the Appendix. Geometrical configurations and fluid properties of exchangers are used to calculate the exchanger pressure drop. Heat duty is used to calculate the exchanger heat transfer area. Then both exchanger pressure drop and heat transfer area are used to calculate the heat transfer coefficients [24].

Furnace fuel used as HEN hot utility reacting with excess air (O_2) produces flue gases including CO_2 . It is assumed that the fuel in the furnace is fuel oil with a carbon content of 87.26% and net heat value NHV of 39,830 kJ/kg is fed at 25 °C with air at the same temperature [30].

4. Results and Discussion

The optimum HRAT value for HEN that corresponds to the lowest total cost can be obtained from the cost targeting profile of Pinch Technology. It is worth mentioning that the total cost is a summation of operation and annualized capital costs. Therefore, heat-shifting options may reveal similar lower total cost but with different HRAT values where the higher is preferred as a heat transfer driving force. Figure 4 illustrates the cost targeting profile for the three options of heat-shifting in the HEN example used in this study. Compared to options 1 and 2, it is clear that option 3 shows the best profile of total capital cost to be lowest at 8.38×10^6 \$/yr corresponds to optimum HRAT of 10 °C. Although the optimum HRAT value shown in the profile of option 1 is 10 °C (similar to that of option 3), but the total cost is higher. In contrast, option 2 illustrates the same trend that is showing a low total cost of 8.5×10^6 \$/yr at lower optimum HRAT value of 6 °C, which can be insufficient heat transfer driving force.

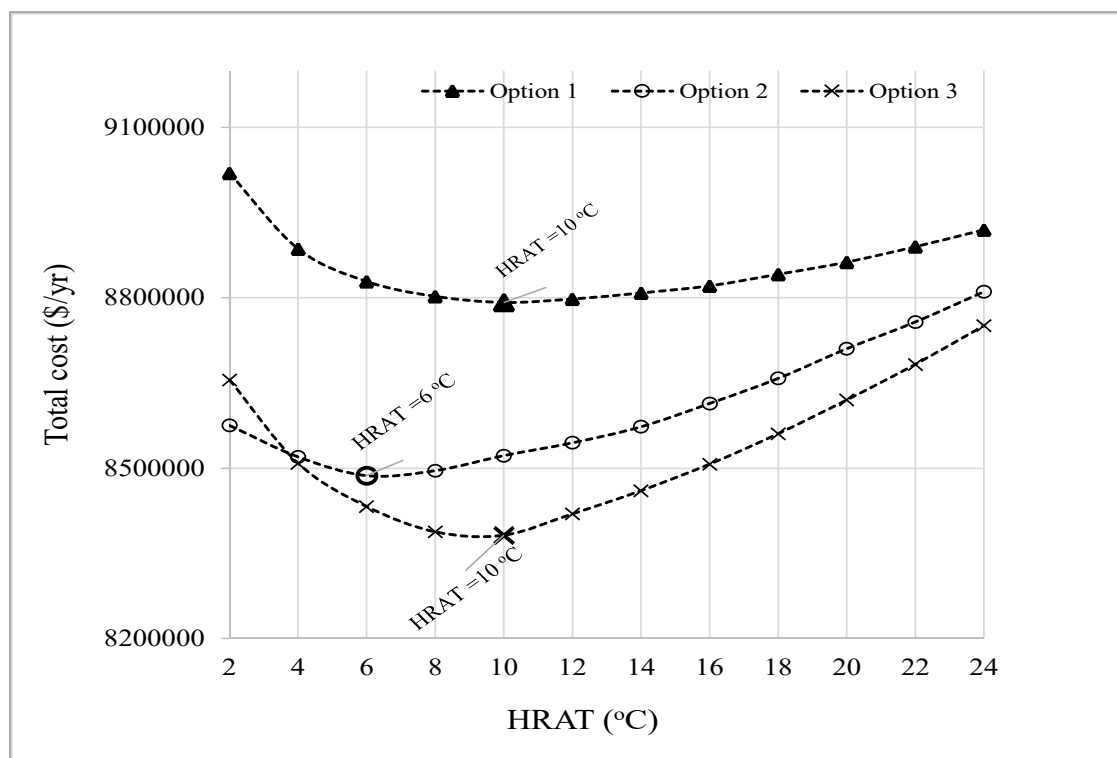


Figure 4. Total cost targeting profile for the three options.

It worth mentioning that option 3 is having the most degrees of freedom where it contained all the HEN paths from A to E. However, the targeting process yields higher total cost for option 3 than option 2 at the lowest HRAT value. That is because option 3 is affecting all HEN exchangers where the additional area is required for them all, and hence increasing the capital and total cost. The Appendix A Tables A11–A13 show a detailed area distribution in HEN using the three options.

The external energy requirements for options 1, 2 and 3 are determined from the energy consumption profiles. Figure 5 shows the energy consumption profile, which has been reduced due to the heat-shifting process at the penalty of additional heat transfer area for options 1, 2 and 3. The pattern of option 3 (a combination of utility paths: A, B, C, D and E in HEN example) indicates the lowest energy consumption and reasonable heat transfer area requirements. Using option 3 at the

optimum HRAT of 10 °C, energy consumption has dropped from 1.34×10^5 kW for the present case to 1.07×10^5 kW, where 2.7×10^4 kW of external energy usage is saved. The additional area requirement is distributed through all the affected exchangers in HEN, which is 5390 m² where it increased from 6960 m² to be 12,350 m² at optimum HRAT value of 10 °C. The area requirement for option 1 is the lowest compared with option 2 and 3; however, energy consumption is trending very high. Option 2 is trending close to option 3 and even better in terms of area requirement, but the optimum HRAT value is low.

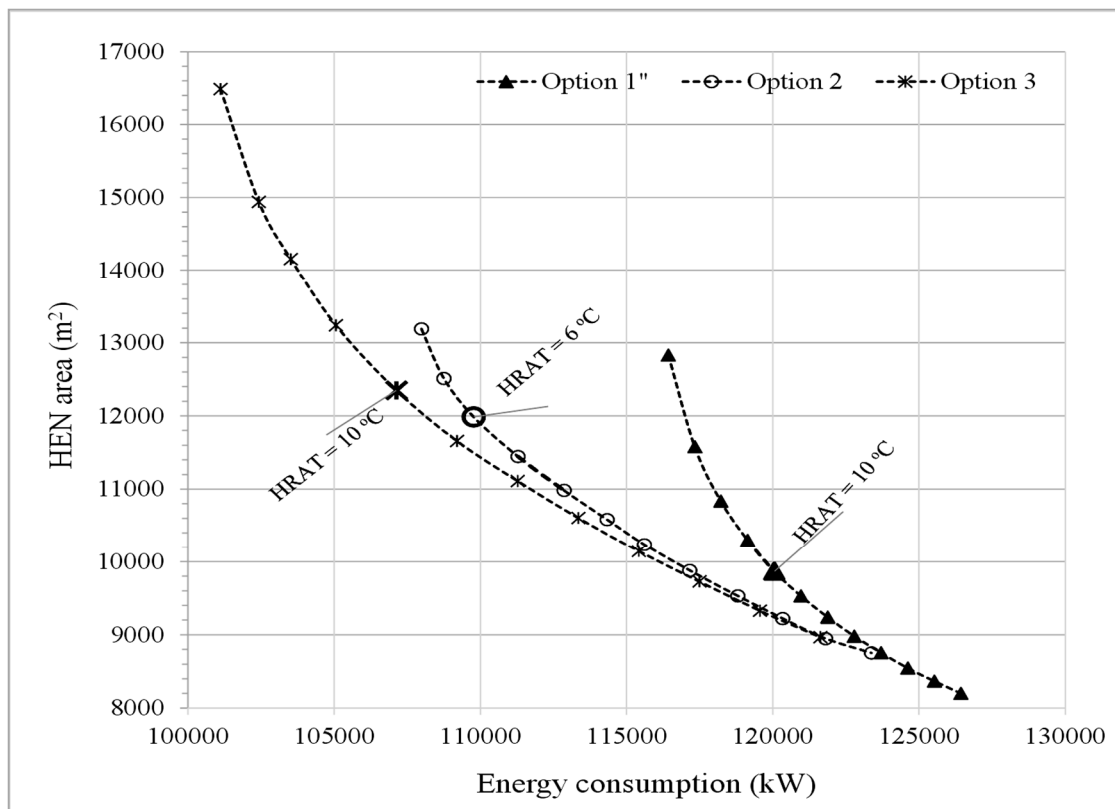


Figure 5. Energy consumption profile with heat transfer area for the three options.

A complete area-energy trade-off can make the right decision to choose the best energy saving option. Therefore, these options are studied economically where the profiles of investment (\$), savings (\$/year), and payback periods (yr) are analyzed concerning HRAT to select the most excellent option.

Figure 6 illustrates the economic profile of option 1. The economic profile shows a gradual decrease in investment, savings, and payback with increasing HRAT. When HRAT increased from 2 °C to the optimum HRAT of 10 °C, the investment cost has dropped by 50%. On the other hand, savings have slightly decreased from 1000K \$/yr to around 800K \$/yr at optimum HRAT. The payback has tremendously decreased from 1.4 yr to approximately 0.86 yr at optimum HRAT of 10 °C.

Figure 7 illustrates the economic profile of option 2. While the ratio of saving to investment started at almost 1 (superimposed saving and investment at HRAT of 2 °C), it became higher with higher HRAT values. Although, this option is showing a short payback period of 0.84 yr, the optimum HRAT of 6 °C makes it insufficient for the heat transfer process between hot and cold streams. This option can be operable by applying some constructional changes in HEN to relax the HRAT value at the expense of higher investment and payback. The constructional changes may include the addition of new HEN devices, exchanger resequencing, and re-piping.

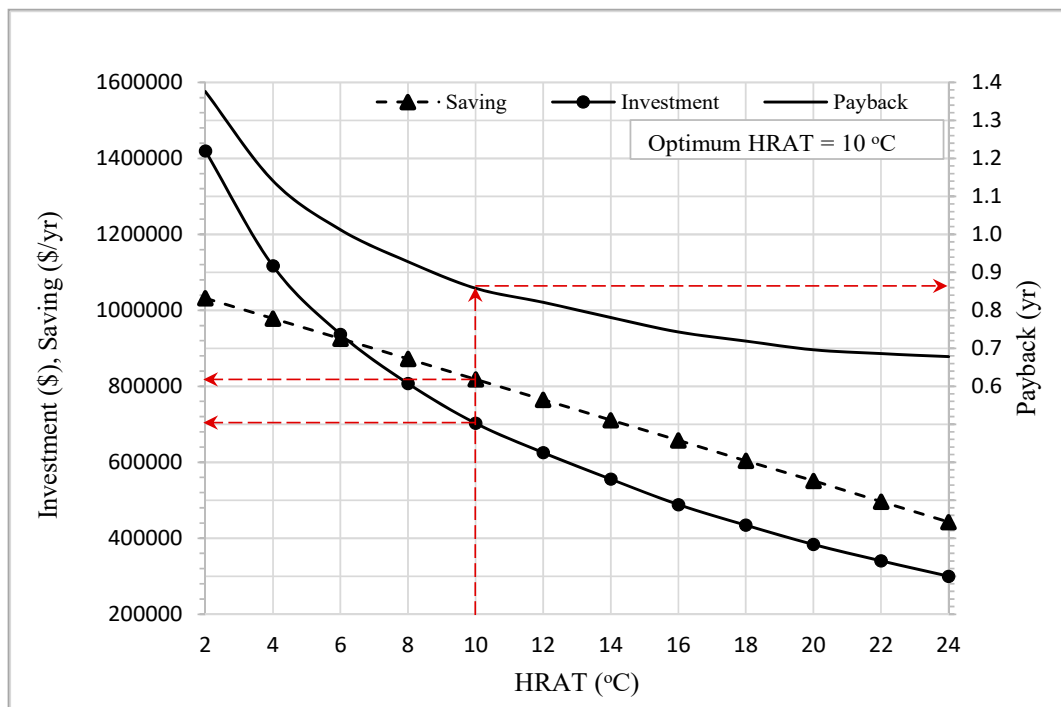


Figure 6. Investment, savings, and payback for option 1.

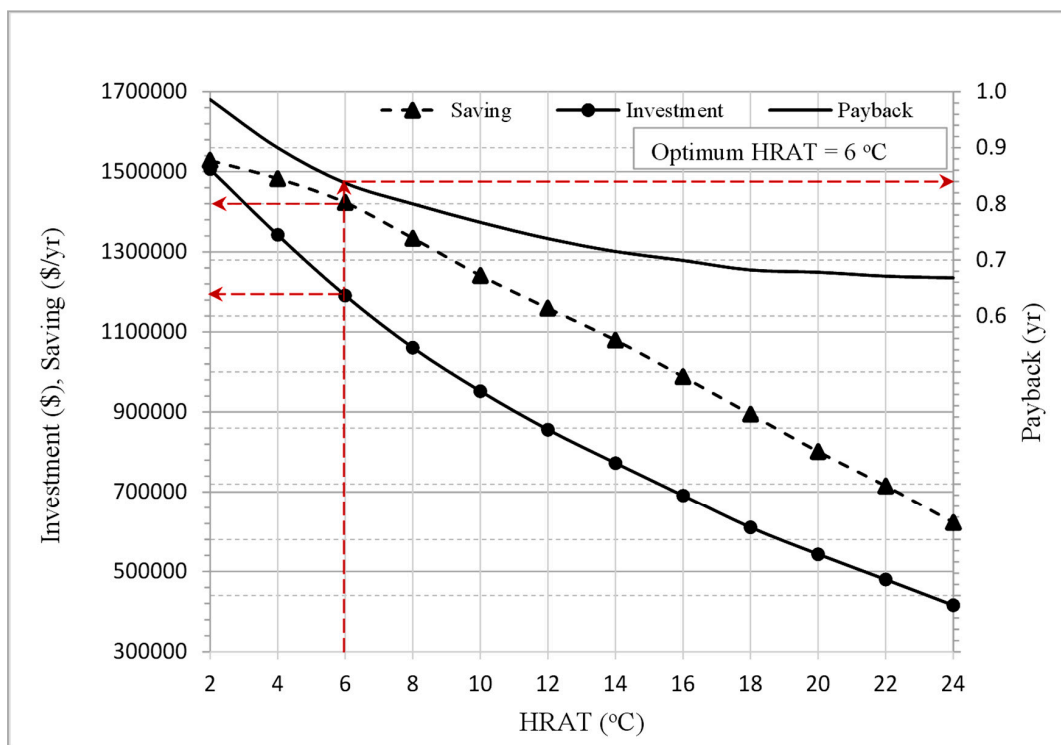


Figure 7. Investment, saving, and payback for option 2.

Figure 8 illustrates the economic profile of option 3. The saving and investment profiles of option 3 are similar to that of option 1. The investment cost profile in this option is lower while the saving profile is higher. As a result, the payback period is fastest with 0.82 yr at the optimum HRAT value. For the HEN case study, option 3 is considered as the best energy saving solution compared to option 1 and 2.

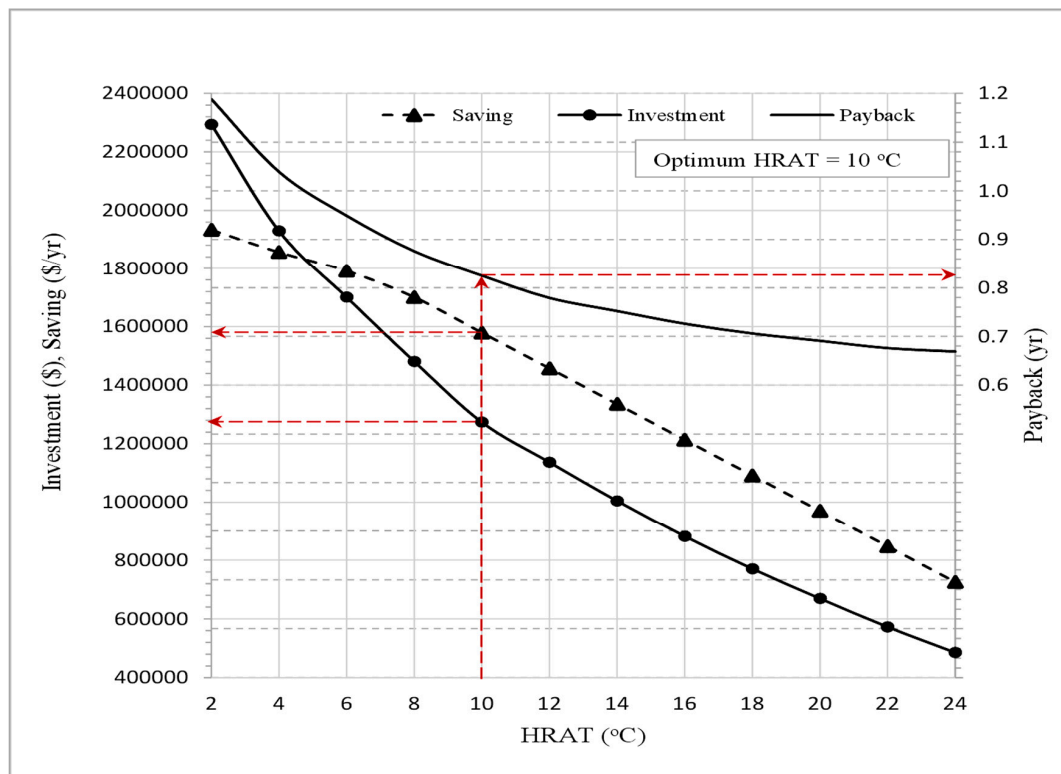


Figure 8. Investment, saving, and payback for option 3.

Also, the effect of reducing energy consumption in HEN on CO₂ emissions is analyzed. The profiles of CO₂ emission along the range of HRAT values for options 1, 2, and 3 are shown in Figure 9. At optimum HRAT, option 3 shows the most CO₂ emission reduction of 17% compared with 15% and 8% for options 2 and 1, respectively. Therefore, option 3 is considered the best environmental option where the annual CO₂ emission from the HEN furnace heater has dropped from 25,190 kg/hr to 20,909 kg/hr at the optimum HRAT of 10 °C.

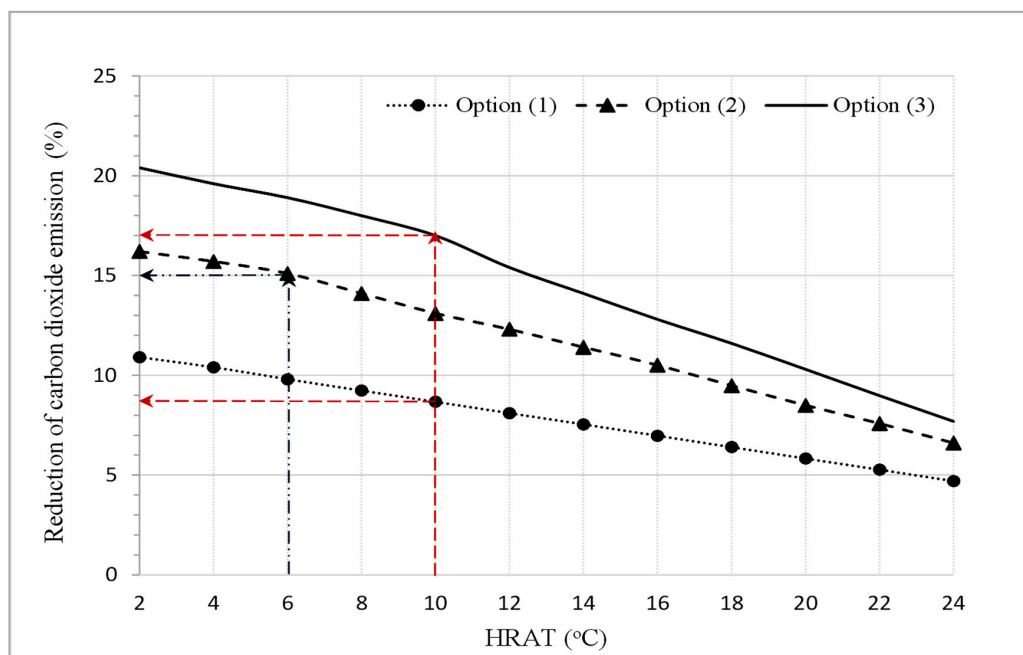


Figure 9. Emission reduction for the three options.

The profiles of CO₂ emission mass flow rate (kg/hr) concerning investment cost for options 1, 2, and 3 are shown in Figure 10. Although option 3 shows a higher investment cost around \$1.3 M, it gives the lowest annual CO₂ emissions of 20,900 kg/hr at optimum HRAT of 10 °C.

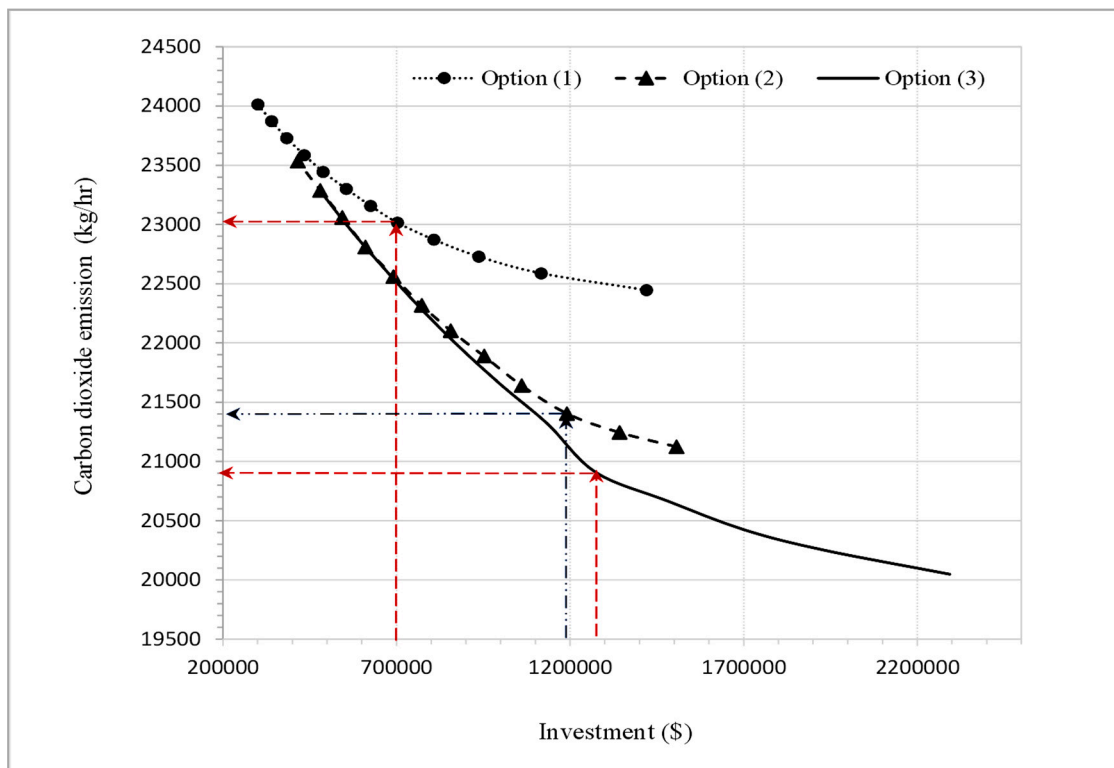


Figure 10. Emission of CO₂ concerning investment for the three options.

5. Conclusions

Heat recovery enhancement is conducted using an approach based on mathematical laws of combination to generate several options of solutions. The present utility paths in the heat exchanger network have combined to successively shift heat load from heaters and coolers to the network exchangers. The heat-shifting process is performed for different values of heat recovery approach temperature while considering the pressure drop in HEN devices. From cost targeting analysis, the best option is selected based on the optimum heat recovery approach temperature. Then, an economic analysis has been performed for the options based on energy saving, investment, and payback period at the optimum heat recovery approach temperature. Finally, CO₂ emission has been evaluated concerning the heat recovery approach temperature and investment. Compared to a previous work done by Osman et al. [24], who introduced paths combination for HEN retrofit at a fixed, the current study considered a wide range of temperature driving force using the cost targeting of Pinch Technology. Moreover, the present study analyses the impact of energy saving on the emission of CO₂ compared to those using paths combination while ignoring the environmental impact such as Awad [14] and Abdelgadir [15].

The real contribution of this study is:

- Merging path combination approach with cost targeting of Pinch Technology to obtain high optimized solutions for energy saving in an existing heat exchanger network and reducing the emission of CO₂.
- The obtained energy saving solutions are considered as low-hanging fruit results where only minor retrofit is considered without topology changes to the network.

The approach adopted for this study is following the concept of Pinch Technology, and it is applied only for simple heat exchanger network such as preheat train unit. Systems that are more complicated can be investigated using the same approach under both Pinch Technology and mathematical programming to generate a hybrid-automated plan.

Author Contributions: Individual contributions of the authors can be specified as: “Conceptualization, A.O.; Formal Analysis & Investigation, M.E.; Methodology, A.O.; Resources, A.O. and M.E.; Supervision & Validation, A.O.; Visualization, A.O. and F.R.; Writing—Original Draft, M.E.; Writing—Review & Editing, A.O. and F.R.”

Funding: This research received no external funding.

Conflicts of Interest: The authors declare no conflict of interest.

Nomenclature

<i>Symbol</i>	<i>Definition</i>
A	Exchanger heat transfer area (m^2).
A_C	Exchanger shell side cross-sectional area (m^2).
$A_{E1}, A_{E2}, A_{E3},$ A_{E4}, A_{E5}, A_{E6}	Heat transfer area for HEN exchangers after heat-shifting (m^2).
$A_{new.HEN}$	Overall heat transfer area of HEN after heat-shifting (m^2).
B_C	Baffle cut (to direct the stream fluid across the tubes).
c	Constant in the tube side pressure drop correlation.
C_P	Specific heat capacity ($kJ/kg \cdot ^\circ C$).
D_s	Shell diameter (m).
d_o	Outside tube diameter (m).
d_I	Inside tube diameter (m).
$E1, E2, E3,$ $E4, E5, E6$	Heat exchanger devices in HEN.
F_I, F_o	Exchanger tube and shell sides flow rate, respectively (m^3/s).
$F_{hw}, F_{hw}, F_{hb},$ F_{hL}, F_{pb}, F_{pl}	Correction factors in the shell side pressure drop correlation.
h_T, h_S	Tube and shell side heat transfer coefficients, respectively ($kW/m^2 \cdot ^\circ C$).
k	Thermal conductivity ($W/m \cdot ^\circ C$).
$K_{PT1}, K_{PT2}, K_{S1}, K_{S2},$ $K_{S3}, K_{hT}, K_{hS}, K_{PS1},$ $K_{PS2}, K_{PS3}, K_{PS4}$	Dimensional constants in the exchanger tube and shell sides pressure drop correlation. They depend on the geometrical configuration and fluid physical properties.
N_T, N_{TP}	Exchanger's number of tubes and number of tube passes, respectively.
PC	Pitch configuration factor.
P_T	Exchanger's tube pitch (center to center distance between adjacent tubes).
Pr	Prandtl number.
$Q_{E1}, Q_{E2}, Q_{E3},$ Q_{E4}, Q_{E5}, Q_{E6}	Exchangers' heat duties (kW) for HEN of the preheat train after heat-shifting.
$Q_{C1}, Q_{C2}, Q_{C3},$ Q_{C4}, Q_{C5}	Cold utilities heat duties (kW) for HEN of the preheat train after heat-shifting.
Q_H	Hot utility heat duty (kW) for HEN of the preheat train after heat-shifting.
ΔP_T	Tube side pressure drop (kPa).
ΔP_S	Shell side pressure drop (kPa).
<i>Greeks</i>	
ρ	Density (kg/m^3).
μ	Viscosity (cP).
v	Velocity (m/s).

Appendix A

All the data in Tables A1–A4 are adopted from Panjishahi and Tahouni [27]. Table A1, shows flow rates and fluid physical properties for crude pre-heat train HEN streams.

Table A1. Flowrates and physical properties for crude oil pre-heat train.

Stream No.	Flow Rate (kg/s)	ρ (kg/m ³)	C_p (J/kg.°C)	μ (cP)	k (W/m.°C)
1	23	700	2600	0.3	0.12
2	44	700	2600	0.4	0.12
3	13	750	2600	0.5	0.12
4	56	750	2600	0.5	0.12
5	253	630	2600	0.2	0.12
6	148	750	2600	0.4	0.12
7	200	800	2600	1.0	0.12

Table A2. Heat exchangers' specifications for heat exchanger networks (HEN) of crude oil pre-heat train.

Geometrical Species	Exchangers					
	E ₁	E ₂	E ₃	E ₄	E ₅	E ₆
P _C	1	1	1	1	1	1
Shell ID(mm)	1143	1219	1143	940	1524	940
Baffle Spacing	509.1	605.1	419.3	197.3	1246.4	255.3
Tube Count	1590	1810	1590	1075	2827	1075
Tube Passes	2	2	2	2	2	2
Tube ID(mm)	15.4	15.4	15.4	15.4	15.4	15.4
Tube OD(mm)	19.1	19.1	19.1	19.1	19.1	19.1
Tube Pitch(mm)	25.4	25.4	25.4	25.4	25.4	25.4
B _C	0.20	0.20	0.25	0.20	0.20	0.25
F _{hn}	1	1	1	1	1	1
F _{hw}	1	1	1	1	1	1
F _{hb}	0.8	0.8	0.8	0.8	0.8	0.8
F _{hl}	0.8	1	0.8	0.8	0.8	0.8
F _{Pb}	1	1	1	1	1	1
F _{PL}	0.5	0.5	1	1	1	0.5
h _{TF}	0.719	0.649	0.758	0.862	0.752	0.763
h _{SF}	0.719	0.649	0.758	0.862	0.752	0.763

Table A3. Exchanger's pressure drop, heat duty, and exchangers' area for existing HEN.

Data	Heat Exchangers					
	E ₁	E ₂	E ₃	E ₄	E ₅	E ₆
ΔP_T (kpa)	53.164	10.776	31.272	32.749	11.549	32.749
ΔP_S (kpa)	26.364	24.357	13.954	4.303	27.859	7.783
Q (kW)	22,000	38,480	15,000	7500	23,000	6000
A (m ²)	1360	2760	800	280	1480	280

Appendix A.1. Heat Recovery Duties

The heat recovery (heat duties for exchangers) after heat-shifting process for option 1, 2 and 3 are tabulated Tables A4–A6.

Table A4. Exchangers heat duties for HEN at different heat recovery approach temperature (HRAT) values using option 1.

HRAT (°C)	Q _{E1} (kW)	Q _{E2} (kW)	Q _{E3} (kW)	Q _{E4} (kW)	Q _{E5} (kW)	Q _{E6} (kW)	Total Heat Recovery (kW)
2	25,435	38,480	20,330	7500	23,000	6000	120,745
4	25,201	38,480	20,112	7500	23,000	6000	120,293
6	24,980	38,480	19,883	7500	23,000	6000	119,843
8	24,753	38,480	19,654	7500	23,000	6000	119,387
10	24,526	38,480	19,425	7500	23,000	6000	118,931
12	24,299	38,480	19,197	7500	23,000	6000	118,476
14	24,072	38,480	18,968	7500	23,000	6000	118,020
16	23,845	38,480	18,739	7500	23,000	6000	117,564
18	23,618	38,480	18,510	7500	23,000	6000	117,108
20	23,390	38,480	18,281	7500	23,000	6000	116,651
22	23,163	38,480	18,053	7500	23,000	6000	116,196
24	22,936	38,480	17,834	7500	23,000	6000	115,750

Table A5. Exchangers heat duties for HEN at different HRAT values using option 2.

HRAT (°C)	Q _{E1} (kW)	Q _{E2} (kW)	Q _{E3} (kW)	Q _{E4} (kW)	Q _{E5} (kW)	Q _{E6} (kW)	Total Heat Recovery (kW)
2	22,000	38,480	18,185	7500	32,800	6000	124,965
4	22,000	38,480	18,000	7500	32,601	6000	124,581
6	22,000	38,480	17,850	7500	32,243	6000	124,073
8	22,000	38,480	17,770	7500	31,567	6000	123,317
10	22,000	38,480	17,700	7500	30,845	6000	122,525
12	22,000	38,480	17,600	7500	30,259	6000	121,839
14	22,000	38,480	17,500	7500	29,674	6000	121,154
16	22,000	38,480	17,425	7500	28,975	6000	120,380
18	22,000	38,480	17,364	7500	28,212	6000	119,556
20	22,000	38,480	17,287	7500	27,522	6000	118,789
22	22,000	38,480	17,200	7500	26,878	6000	118,058
24	22,000	38,480	17,129	7500	26,160	6000	117,269

Table A6. Exchangers heat duties for HEN at different HRAT values using option 3.

HRAT (°C)	Q _{E1} (kW)	Q _{E2} (kW)	Q _{E3} (kW)	Q _{E4} (kW)	Q _{E5} (kW)	Q _{E6} (kW)	Total Heat Recovery (kW)
2	22,461	38,480	17,342	8300	32,870	8950	128,403
4	22,312	38,480	17,194	8140	32,770	8850	127,746
6	22,120	38,480	16,940	8100	32,740	8820	127,200
8	22,015	38,480	16,740	7900	32,560	8735	126,430
10	22,013	38,480	16,172	7860	32,340	8530	125,395

Table A6. Cont.

HRAT (°C)	Q _{E1} (kW)	Q _{E2} (kW)	Q _{E3} (kW)	Q _{E4} (kW)	Q _{E5} (kW)	Q _{E6} (kW)	Total Heat Recovery (kW)
12	22,011	38,480	16,079	7820	31,870	8100	124,360
14	22,010	38,480	16,049	7790	30,913	8080	123,322
16	22,009	38,480	16,000	7730	30,076	7990	122,285
18	22,007	38,480	15,932	7692	29,260	7879	121,250
20	22,005	38,480	15,909	7640	28,340	7841	120,215
22	22,004	38,480	15,882	7610	27,480	7722	119,178
24	22,002	38,480	15,878	7560	26,560	7663	118,143

Appendix A.2. Energy Consumption

Energy CONSUMPTION (heat duties of hot and cold utility devices) after the heat-shifting for HEN using options 1, 2, and 3 at different HRAT values are tabulated in Tables A7–A9.

Table A7. Hot and cold utilities heat duties for HEN at different HRAT values using option 1.

HRAT (°C)	Q _H (kW)	Q _{C1} (kW)	Q _{C2} (kW)	Q _{C3} (kW)	Q _{C4} (kW)	Q _{C5} (kW)	Total Utility Requirement (kW)
2	71,655	2970	5982	3316	22,613	9890	116,426
4	72,107	2970	6200	3316	22,847	9890	117,330
6	72,557	2970	6429	3316	23,058	9890	118,220
8	73,013	2970	6658	3316	23,295	9890	119,142
10	73,469	2970	6887	3316	23,522	9890	120,054
12	73,924	2970	7115	3316	23,749	9890	120,964
14	74,380	2970	7344	3316	23,976	9890	121,876
16	74,835	2970	7573	3316	24,202	9890	122,786
18	75,292	2970	7802	3316	24,430	9890	123,700
20	75,749	2970	8031	3316	24,658	9890	124,614
22	76,204	2970	8259	3316	24,885	9890	125,524
24	76,660	2970	8488	3316	25,112	9890	126,436

Table A8. Hot and cold utilities heat duties for HEN at different HRAT values using option 2.

HRAT (°C)	Q _H (kW)	Q _{C1} (kW)	Q _{C2} (kW)	Q _{C3} (kW)	Q _{C4} (kW)	Q _{C5} (kW)	Total Utility Requirement (kW)
2	67,435	2970	8127	3316	26,048	90	107,986
4	67,819	2970	8312	3316	26,048	289	108,754
6	68,327	2970	8462	3316	26,048	647	109,770
8	69,083	2970	8542	3316	26,048	1323	111,282
10	69,875	2970	8612	3316	26,048	2045	112,866
12	70,561	2970	8712	3316	26,048	2721	114,328
14	71,246	2970	8812	3316	26,048	3216	115,608
16	72,020	2970	8887	3316	26,048	3915	117,156
18	72,844	2970	8948	3316	26,048	4678	118,804
20	73,611	2970	9025	3316	26,048	5368	120,338
22	74,342	2970	9112	3316	26,048	6012	121,800
24	75,131	2970	9183	3316	26,048	6730	123,378

Table A9. Hot and cold utilities heat duties for HEN at different HRAT values using option 3.

HRAT (°C)	Q _H (kW)	Q _{C1} (kW)	Q _{C2} (kW)	Q _{C3} (kW)	Q _{C4} (kW)	Q _{C5} (kW)	Total Utility Requirement (kW)
2	63,997	20	8970	2516	25,587	20	101,110
4	64,654	120	9118	2676	25,736	120	102,424
6	65,200	150	9372	2716	25,928	150	103,516
8	65,970	235	9572	2916	26,033	330	105,056
10	67,005	440	10140	2956	26,035	550	107,126
12	68,040	870	10,233	2996	26,037	1020	109,196
14	69,078	890	10,263	3026	26,038	1977	111,272
16	70,115	980	10,312	3086	26,039	2814	113,346
18	71,150	1091	10,380	3124	26,041	3630	115,416
20	72,188	1129	10,403	3176	26,043	4550	117,489
22	73,222	1248	10,430	3206	26,044	5410	119,560
24	74,257	1307	10,434	3256	26,046	6330	121,630

As per Nie and Zhu [28], Smith [31] and Osman et al. [24], the heat transfer coefficients for tube side and shell side can be obtained while considering the exchanger pressure drop. The dimensional constants in the pressure drop Equations (6) and (7) are calculated as follows:

$$K_{PT1} = \frac{0.023 \cdot \rho^{0.8} \cdot \mu^{0.2} \cdot d_I^{0.8}}{F_I \cdot d_o} \cdot \left(\frac{1}{K_{hT}} \right)^{3.5} \quad (\text{A1})$$

$$F_I = \frac{\pi \cdot d_I^2}{4} \cdot N_{TP} \cdot v \quad (\text{A2})$$

$$K_{PT2} = 1.25 N_{TP} \cdot \rho \cdot \left(\frac{1}{K_{hT}} \right)^{2.5} \quad (\text{A3})$$

$$N_T = \frac{\frac{\pi}{4} \cdot D_S^2}{P_C \cdot P_T^2} \quad (\text{A4})$$

$$K_{hT} = c \cdot \left(\frac{k}{d_I} \right) \cdot Pr^{\frac{1}{3}} \cdot \left(\frac{d_I \cdot \rho}{\mu} \right)^{0.8} \quad (\text{A5})$$

$$Pr = \frac{C_P \cdot \mu}{k} \quad (\text{A6})$$

$$K_{S1} = \frac{2 \cdot K_{PS1} - K_{PS3}}{K_{hS}^{2.86}} \quad (\text{A7})$$

$$K_{S2} = \frac{K_{PS2}}{K_{hS}^{4.42}} \quad (\text{A8})$$

$$K_{S3} = \frac{K_{PS4}}{K_{hS}^{4.69}} \quad (\text{A9})$$

$$K_{PS1} = \frac{1.298 \cdot F_{pb} \cdot (1 - B_C) \cdot D_S \cdot \rho^{0.83} \cdot \mu^{0.17}}{P_T d_o^{0.17}} \quad (\text{A10})$$

$$K_{PS2} = \frac{0.5261 \cdot F_{pb} \cdot F_{pL} \cdot P_C \cdot (1 - 2 \cdot B_C) \cdot (P_T - d_o) \cdot \rho^{0.83} \cdot \mu^{0.17}}{F_o d_o^{1.17}} \quad (\text{A11})$$

$$K_{PS3} = \frac{2.596 \cdot F_{pb} \cdot F_{pL} \cdot (1 - 2 \cdot B_C) \cdot D_S \cdot \rho^{0.83} \cdot \mu^{0.17}}{P_T d_o^{1.17}} \quad (\text{A12})$$

$$K_{PS4} = \frac{0.2026 \cdot F_{pL} \cdot P_C \cdot P_T \cdot (P_T - d_o) \cdot \rho}{F_o d_o} \cdot \left(\frac{2}{D_S} + \frac{0.6 \cdot B_C}{P_T} \right) \quad (\text{A13})$$

$$K_{hS} = \frac{0.24 \cdot F_{lm} \cdot F_{hw} \cdot F_{hb} \cdot F_{hL} \cdot \rho^{0.64} \cdot C_p^{0.333} \cdot k^{0.667}}{\mu^{0.307} d_o^{0.36}} \quad (\text{A14})$$

$$F_o = v \cdot A_C \quad (\text{A15})$$

$$A_C = \left(\frac{P_T - d_o}{P_T} \right) \cdot D_S \cdot L_B \quad (\text{A16})$$

Consequently, the obtained heat transfer coefficient for tube and shell sides of all the affected exchangers at optimum HRAT for the heat-shifting options are tabulated in Table A10 below:

Table A10. Heat transfer coefficients for exchangers' tube and shell sides (kW/m²·°C) of the affected exchangers in HEN for option 1, 2 and 3 at optimum HRAT.

Heat-Shifting Options	Optimum HRAT (°C)	E1		E2		E3		E4		E5		E6	
		<i>h_T</i>	<i>h_S</i>										
1	10	0.342	0.456	0.35	0.433	0.325	0.451	-	-	-	-	-	-
2	6	-	-	-	-	0.331	0.463	0.346	0.432	0.324	0.531	0.333	0.511
3	10	0.35	0.467	0.35	0.433	0.337	0.473	0.348	0.436	0.324	0.531	0.335	0.514

Appendix A.3. Heat Transfer Area Distribution

For each exchanger in HEN of the preheat train after heat-shifting, the actual heat transfer area at different HRAT values, is tabulated in Tables A11–A13 for options 1, 2, and 3. Also, the overall heat transfer area for the existing HEN is presented in the same tables for the selected options.

Table A11. Heat transfer area for HEN exchangers after heat-shifting, using option 1.

HRAT (°C)	A _{E1} (m ²)	A _{new,HEN} (m ²)					
2	4349	3155	3288	280	1480	280	12,832
4	3619	3138	2782	280	1480	280	11,579
6	3210	3116	2470	280	1480	280	10,836
8	2913	3099	2246	280	1480	280	10,298
10	2677	3078	2071	280	1480	280	9866
12	2499	3062	1929	280	1480	280	9530
14	2345	3045	1810	280	1480	280	9240
16	2210	3025	1706	280	1480	280	8981
18	2092	3009	1615	280	1480	280	8756
20	1984	2989	1533	280	1480	280	8546
22	1894	2974	1460	280	1480	280	8368
24	1809	2958	1394	280	1480	280	8201

Table A12. Heat transfer area for HEN exchangers after heat-shifting, using option 2.

HRAT (°C)	A _{E1} (m ²)	A _{new,HEN} (m ²)					
2	2474	3965	3203	365	2903	280	13,190
4	2416	3917	2669	363	2866	280	12,511
6	2339	3850	2360	360	2798	280	11,987
8	2236	3755	2145	354	2677	280	11,447
10	2155	3664	1981	348	2553	280	10,981
12	2072	3588	1848	343	2453	280	10,584
14	2006	3516	1736	339	2361	280	10,238
16	1936	3436	1641	334	2253	280	9880
18	1869	3355	1558	328	2140	280	9530
20	1810	3282	1485	324	2041	280	9222
22	1759	3217	1419	319	1954	280	8948
24	1709	3151	1360	315	1935	280	8750

Table A13. Heat transfer area for HEN exchangers after heat-shifting, using option 3.

HRAT (°C)	A _{E1} (m ²)	A _{new,HEN} (m ²)					
2	4174	4406	3151	760	3134	862	16,487
4	3467	4330	2623	604	3101	813	14,938
6	3149	4272	2262	579	3094	799	14,155
8	2769	4170	1998	490	3049	764	13,240
10	2556	4022	1626	469	2986	691	12,350
12	2386	3884	1514	444	2854	577	11,659
14	2243	3755	1435	423	2684	572	11,112
16	2122	3635	1362	399	2535	553	10,606
18	2017	3528	1292	382	2397	531	10,147
20	1924	3421	1239	364	2256	524	9728
22	1841	3322	1188	351	2125	502	9329
24	1767	3227	1150	336	1996	492	8968

The parameters and symbols used in the Appendix equations and tables are defined as in the nomenclature Table below.

References

1. Linnhoff, B.; Turner, J. Heat-recovery networks, new insights yield big savings. *Chem. Eng.* **1981**, *88*, 56–70.
2. Linnhoff, B.; Townsend, D.W.; Boland, D.; Hewitt, G.F.; Thomas, B.E.A.; Guy, A.R.; Marsland, R.H. *A User Guide to Process Integration for the Efficient Use of Energy*, 1st ed.; IChemE: Rugby, UK, 1983.
3. Linnhoff, B. Pinch technology has come of age. *Chem. Eng. Progr.* **1984**, *80*, 33–40.
4. Tjoe, T.N.; Linnhoff, B. Using pinch technology for process retrofit. *Chem. Eng.* **1986**, *93*, 47–60.
5. Gadalla, M.A.; Olujić, Z.; Jansens, P.J.; Jobson, M.; Smith, R. Reducing CO₂ emissions and energy consumption of heat-integrated distillation systems. *Environ. Sci. Technol.* **2005**, *39*, 6860–6870. [[CrossRef](#)] [[PubMed](#)]

6. Biyanto, T.R.; Gonawan, E.K.; Nugroho, G.; Hantoro, R.; Cordova, H.; Indrawati, K. Heat exchanger network retrofit throughout overall heat transfer coefficient by using genetic algorithm. *Appl. Therm. Eng.* **2016**, *94*, 274–281. [[CrossRef](#)]
7. Ayotte-Sauvé, E.; Ashrafi, O.; Rohani, N. Optimal retrofit of heat exchanger networks, A stepwise approach. *Comput. Chem. Eng.* **2017**, *106*, 243–268. [[CrossRef](#)]
8. Kang, L.; Liu, Y. Synthesis of flexible heat exchanger networks, A review. *Chin. J. Chem. Eng.* **2018**. [[CrossRef](#)]
9. Varbanov, P.S.; Klemes, J. Rules of Path Construction for HEN Debottlenecking. *Appl. Therm. Eng.* **2000**, *20*, 1409–1420. [[CrossRef](#)]
10. Van Reisen, J.L.; Grievink, J.; Polley, G.T.; Verheijen, P.J. The placement of two-stream and multi-stream heat-exchangers in an existing network through path analysis. *Comput. Chem. Eng.* **1995**, *19*, 143–148. [[CrossRef](#)]
11. Van Reisen, J.L.; Polley, G.T.; Verheijen, P.J. Structural targeting for heat integration retrofit. *Appl. Therm. Eng.* **1998**, *18*, 283–294. [[CrossRef](#)]
12. Osman, A. Paths Analysis for the Retrofit of Heat Exchanger Networks and the Utility System. Ph.D. Thesis, Universiti Teknologi PETRONAS, Perak, Malaysia, 2011.
13. Osman, A.; Mutalib, M.A.; Shigidi, I. Heat recovery enhancement in HEN using a combinatorial approach of paths combination and process streams' temperature flexibility. *S. Afr. J. Chem. Eng.* **2016**, *21*, 37–48. [[CrossRef](#)]
14. Awad, M. Energy Optimization and Retrofit of Heat Exchanger Networks. Master's Thesis, University of Gezira, Wad Medani, Sudan, 2013.
15. Abdelgadir, K. Determination of the Optimum Heat Recovery Approach Temperature for an Existing Heat Exchanger Network of Crude Distillation Unit. Master's Thesis, University of Gezira, Wad Medani, Sudan, 2014.
16. Polley, G.T.; Panjeshahi, M.H.; Jegede, F.O. Pressure Drop Consideration in the Retrofit of Heat Exchanger Networks. *Trans. IChemE* **1990**, *68*, 211–220.
17. Panjeshahi, M.H. Pressure Drop Consideration in Process Integration. Ph.D. Thesis, The University of Manchester Institute of Science and Technology (UMIST), Manchester, UK, 1992.
18. Marcone, L.S.; Zemp, J.R. Retrofit of Pressure Drop Constrained Heat Exchanger Network. *Appl. Therm. Eng.* **2000**, *20*, 1469–1480.
19. Gadalla, M.A. Retrofit Design of Heat-Integrated Crude Oil Distillation Systems. Ph.D. Thesis, The University of Manchester Institute of Science and Technology (UMIST), Manchester, UK, 2003.
20. Lai, Y.Q.; Alwi, S.R.W.; Manan, Z.A. Customized retrofit of heat exchanger network combining area distribution and targeted investment. *Energy* **2019**, *179*, 1054–1066. [[CrossRef](#)]
21. Steyn, P. Global environmental management, an exploration of the world summit on sustainable development. *J. Contemp. Hist.* **2002**, *27*, 1–13.
22. Climate Change and Sustainability. John Ray Initiative. Available online: <https://www.wheaton.edu/media/migrated-images-amp-files/media/files/centers-and-institutes/cace/articles/GWHoughton.pdf> (accessed on 10 August 2018).
23. Kang, L.; Liu, Y. A systematic strategy for multi-period heat exchanger network retrofit under multiple practical restrictions. *Chin. J. Chem. Eng.* **2017**, *25*, 1043–1051. [[CrossRef](#)]
24. Osman, A.; Mutalib, M.A.; Shuhaimi, M.; Amminudin, K. Paths combination for HEN retrofit. *Appl. Therm. Eng.* **2009**, *29*, 3103–3109. [[CrossRef](#)]
25. Swokowski, W.E.; Cole, A.J. *Precalculus, Functions and Graphs*, 10th ed.; Thomson Learning Academic Resource Center: Toronto, ON, Canada, 2005.
26. Martin, A.; Mato, F.A. An educational software for heat exchanger network design with the pinch method. *Educ. Chem. Eng.* **2008**, *3*, e6–e14. [[CrossRef](#)]
27. Nie, X.; Zhu, X. Heat exchanger network retrofit considering pressure drop and heat-transfer enhancement. *AIChE J.* **1999**, *45*, 239–1254. [[CrossRef](#)]
28. Al-Riyami, B.A.; Klemeš, J.; Perry, S. Heat integration retrofit analysis of a heat exchanges network of a fluid catalytic cracking plant. *Appl. Therm. Eng.* **2001**, *21*, 449–1487. [[CrossRef](#)]
29. Panjeshahi, M.H.; Tahouni, N. Pressure drop optimization in debottlenecking of heat exchanger networks. *Energy* **2008**, *33*, 942–951. [[CrossRef](#)]

30. Mahmoud, A.; Shuhaimi, M.; Samed, M.A. A combined process integration and fuel switching strategy for emissions reduction in chemical process plants. *Energy* **2009**, *34*, 190–195. [[CrossRef](#)]
31. Smith, R. *Chemical Process Design and Integration*, 2nd ed.; John Wiley & Sons Ltd.: Sussex, UK, 2005.



© 2019 by the authors. Licensee MDPI, Basel, Switzerland. This article is an open access article distributed under the terms and conditions of the Creative Commons Attribution (CC BY) license (<http://creativecommons.org/licenses/by/4.0/>).